THE JOURNAL OF BIOLOGICAL CHEMISTRY VOL. 287, NO. 35, pp. 30024–30034, August 24, 2012

Modulation of Dynamin-related Protein 1 (DRP1) Function by Increased *O*-linked-β-*N*-acetylglucosamine Modification (*O*-GlcNAc) in Cardiac Myocytes*

Received for publication, June 12, 2012, Published, JBC Papers in Press, June 28, 2012, DOI 10.1074/jbc.M112.390682

Thomas Gawlowski[‡], Jorge Suarez[‡], Brian Scott[‡], Moises Torres-Gonzalez[‡], Hong Wang[‡], Raphaela Schwappacher[‡], Xuemei Han[§], John R. Yates III[§], Masahiko Hoshijima[‡¶], and Wolfgang Dillmann[‡1]

From the [‡]Department of Medicine, [¶]Center for Research in Biological Systems, University of California, San Diego, La Jolla, California 92039 and the [§]Department of Chemical Physiology, The Scripps Research Institute, La Jolla, California 92037

Background: DRP1 plays a significant role to control mitochondrial fission.
Results: DRP1 is *O*-GlcNAcylated. Increased *O*-GlcNAcylation augments the level of the GTP-bound active form of DRP1 and induces translocation of DRP1 from cytoplasm to mitochondria.
Conclusion: *O*-GlcNAcylation modulates DRP1 function, which has consequences for mitochondrial function.
Significance: The modulation of DRP1 function by increased overall *O*-GlcNAcylation could play a significant role in the development of diabetic mitochondrial dysfunction.

***O*-linked-*N*-acetyl-glucosamine glycosylation (*O*-GlcNAcylation) of the serine and threonine residues of cellular proteins is a dynamic process and affects phosphorylation. Prolonged *O*-GlcNAcylation has been linked to diabetes-related complications, including mitochondrial dysfunction. Mitochondria are dynamically remodeling organelles, that constantly fuse (fusion) and divide (fission). An imbalance of this process affects mitochondrial function. In this study, we found that dynamin-related protein 1 (DRP1) is *O*-GlcNAcylated in cardiomyocytes at threonine 585 and 586. *O*-GlcNAcylation was significantly enhanced by the chemical inhibition of *N*-acetyl-glucosaminidase. Increased *O*-GlcNAcylation decreases the phosphorylation of DRP1 at serine 637, which is known to regulate DRP1 function. In fact, increased *O*-GlcNAcylation augments the level of the GTP-bound active form of DRP1 and induces translocation of DRP1 from the cytoplasm to mitochondria. Mitochondrial fragmentation and decreased mitochondrial membrane potential also accompany the increased *O*-GlcNAcylation. In conclusion, this report shows, for the first time, that *O*-GlcNAcylation modulates DRP1 functionality in cardiac muscle cells.**

Recent studies have identified that mitochondria fuse and divide dynamically and that such dynamic remodeling is critical to maintain proper mitochondrial function (1, 2). Although several dynamin-related GTPases regulate these processes, dynamin-related protein 1 (DRP1)[2] plays a significant role to control mitochondrial fission (3). Although involved in mitochondrial function, DRP1 is mostly localized in cytoplasm with ~3% associated with the mitochondrial membrane at rest under physiological conditions (4). The functional properties of DRP1 are modulated by a number of posttranslational modifications, including phosphorylation (5–7), SUMOylation (8), ubiquitination (9), and *S*-nitrosylation (10). DRP1 is phosphorylated at two sites, serine 616 (Ser-616 and 637 Ser-637, referring to the sequence of the human DRP1), which are well conserved (5, 11, 12). Phosphorylation of Ser-616 by cyclin-dependent kinase 1 and dephosphorylation of Ser-637 by calcineurin promote mitochondrial fission. The impact of Ser-637 phosphorylation on mitochondrial function has been a focus of most prior investigations. Cereghetti *et al.* (7) have shown that calcineurin, a Ca-dependent protein phosphatase, dephosphorylates Ser-637, resulting in the translocation of DRP1 from cytoplasm to mitochondria. The mitochondrial outer membrane proteins FIS1 and mitochondrial fission factor recruit DRP1 to the mitochondrial outer membrane (13–15).

O-linked *N*-acetyl-glucosamine glycosylation (*O*-GlcNAcylation) posttranslationally modifies nuclear, cytosolic, and mitochondrial proteins occurring on serine and threonine residues (16–18). *O*-GlcNAcylation and phosphorylation sites overlap, so these two reactions have reciprocal effects on protein function (19). In mammalian cells, protein *O*-GlcNAcylation is regulated by the opposing actions of two enzymes: the *O*-GlcNAc-transferase, which catalyzes the addition of *O*-linked *N*-acetyl-glucosamine (*O*-GlcNAc) and the *N*-acetyl-glucosaminidase (OGA), which removes *O*-GlcNAc residues. A shorter splice variant of *O*-GlcNAc-transferase has been identified that exhibits preferred mitochondrial localization (20). In diabetes,

* This work was supported, in whole or in part, by National Institutes of Health Grants HL066917 (to W. H. D.), 3R01HL066917-10S1 (to J. S.), P41 RR011823 (to J. R. Y.), P60 MD00220 from the San Diego EXPORT Center, National Center of Minority Health and Health Disparities, and the UCSD Neuroscience Microscopy Facility grant P30 NS047101. This work was also supported by a grant from the Deutsche Forschungsgemeinschaft (to T. G.) and by the P. Robert Majumder Charitable Foundation.
[1] To whom correspondence should be addressed: Division of Endocrinology and Metabolism, Department of Medicine, University of California, San Diego, 9500 Gilman Drive, La Jolla, CA 92039-0618. Tel.: 858-534-9934; Fax: 858-534-9932; E-mail: wdillmann@ucsd.edu.

[2] The abbreviations used are: DRP1, dynamin-related protein 1; OGA, *N*-acetyl-glucosaminidase; PUGNAc, *O*-(2-Acetamido-2-deoxy-D-glucopyranosylidenamino) *N*-phenylcarbamate; a.u., arbitrary units; *O*-GlcNAc, *O*-linked-*N*-acetyl-glucosamine glycosylation; NCM, neonatal rat cardiomyocyte; HG, high glucose; NG, normal glucose.

increased *O*-GlcNAcylation of a set of cytoplasmatic and nuclear proteins has been shown, which is likely due to the activation of the hexosamine biosynthetic pathway (18, 21–23). Consistent with these observations, we found that several mitochondrial proteins are highly *O*-GlcNAcylated in cardiomyocytes exposed to high glucose (18, 24). High glucose treatment also resulted in augmented mitochondrial fragmentation and decreased mitochondrial membrane potential (24). In our previous work we demonstrated that the reduced expression of a fusion-related mitochondrial protein OPA1 and its increased *O*-GlcNAcylation are at least partly the cause of mitochondrial fragmentation in cardiac myocytes exposed to high glucose (24). As fission counteracts fusion to control the level of mitochondrial fragmentation, this study investigated whether *O*-GlcNAcylation occurs in the fission-related protein DRP1 and if increased *O*-GlcNAcylation affects the functionality of DRP1. Our results show that DRP1 is *O*-GlcNAcylated in neonatal cardiomyocytes and that the *O*-GlcNAcylation of DRP1 is increased by OGA inhibition. In addition, excessive overall *O*-GlcNAcylation decreases phosphorylation of DRP1 at Ser-637, increases its GTP-binding, and translocates DRP1 to mitochondria. Furthermore, we found that increased protein *O*-GlcNAcylation by OGA inhibition augments mitochondrial fragmentation and impairs mitochondrial function in cardiomyocytes.

EXPERIMENTAL PROCEDURES

Materials—Low-glucose DMEM, M199, MitoTracker Green FM, and JC-1 were purchased from Invitrogen. The following antibodies were used: DRP1 (BD Biosciences), porin (Cell Signaling Technology), FIS1 (Invitrogen), phospho-Ser-637-DRP1 (Cell Signaling Technology), RL2 anti-*O*-GlcNAc antibody (Thermo Scientific), anti-rabbit Alexa Flour 488 and anti-mouse Alexa Flour 568 (Invitrogen), and anti-mouse and anti-rabbit IgG-HRP-conjugated antibodies (Thermo Scientific). Wheat germ agglutinin (WGA)-conjugated beads were purchased from Vector Laboratories. The OGA inhibitor PUGNAc was purchased from Toronto Research Chemicals.

Type 2 Diabetic Mouse Model—All animal protocols were approved by the University of California, San Diego, Institutional Animal Care and Use Committee and conform to the Guide for the Care and Use of Laboratory Animals as outlined by the NIH. Eight-week old C57BL/6 mice were injected once intraperitoneally with streptozotocin (STZ) (75 mg/kg) and placed on high fat diet (HFD; Harlan, 60% fat) for 4 months. C57BL/6 mice on normal chow were used as controls.

Adenoviral Vector—The cDNA corresponding to the human OGA was kindly provided by G. Hart (25). This cDNA was inserted into the E1 region of an adenoviral shuttle vector. Replication deficient adenovirus particles with OGA (Adv-OGA) or without (Adv-control) were generated by recombination in 293 cells, single plaques were isolated, and propagated to achieve high titer. Adenoviral particles were CsCl-purified and quantified by plaque titer assay.

Cell Culture and Treatment—Primary cultures of neonatal rat cardiomyocytes (NCMs) were prepared as described previously (18). Cells were plated onto gelatin-coated culture dishes. Plating medium consisted of 4.25:1 L-DMEM: M199, 10% horse serum, 5% fetal bovine serum, 1% penicillin/streptomycin/fungizone. Cells were allowed to adhere to the plates for 24 h before changing to basic experimental culture medium (4.5:1 L-DMEM: M199, 2% fetal bovine serum, 1% penicillin/streptomycin/fungizone). For high glucose treatment (HG), 20 mM glucose was added to the media (the final glucose concentration was 25 mM). In a control group of cells, equimolar mannitol was added to exclude the potential effect of changes in osmolarity (normal glucose [NG]: glucose concentration, 5 mM). NCMs exposed to high glucose were also treated with Adv-OGA or Adv-control. NCMs were infected at a multiplicity of infection of 50 pfu/cell for 24 h. Then, NCMs were washed and treated with NG (5 mM) or HG (25 mM) for 72 h The culture medium was changed daily until the cells were harvested. For OGA inhibition, cells were treated with 100 μM PUGNAc or 100 nM Thiamet G or the vehicle ethanol, as control, overnight.

Subcellular Fractions—After treatment, cells were collected using the lysis buffer (10 mM Tris pH 7.4, 0.25 M mM sucrose, 3 mM $MgCl_2$, 1 mM β-glycerolphosphate, 2.5 mM Na-pyrophosphate, Na_3-VO_4, 10% glycerol, 0.025 mM PUGNAc, 1:1000 diluted protease and phosphase inhibitor mixture). Lysates were centrifuged at 1000 $\times$ *g* for 10 min at 4 °C. The supernatant was spun at 10,000 $\times$ *g* for 10 min at 4 °C, yielding a mitochondria-enriched pellet. The supernatant was spun at 100,000 $\times$ *g* for 60 min at 4 °C to yield cytosol. Equal protein amounts from each fraction were analyzed by Western blotting.

Immunohistochemistry—Cells were grown on glass coverslips. After treatment, cells were washed once with PBS and fixed with ice cold ethanol (100% v/v) for 15 min at room temperature. To suppress unspecific labeling the cells were incubated with blocking solution (1% BSA, 1% chicken serum, 1% goat serum, and 0.1% Triton X-100 in PBS) for 1 h at room temperature. Mouse anti-DRP1 (1:300) and rabbit anti-FIS1 (1:300) antibodies in 1% BSA solution (in PBS, pH 7.4) were added for 1 h at room temperature. After three washes with PBS the secondary antibodies conjugated with Alexa Flour 488 or Alexa Flour 568 (1:300) were added for 1 h at room temperature. After three washes with PBS, coverslips were mounted using mounting medium (Vector Lab. Inc.).

GTP-binding Assay—The GTP-binding assay was performed according to the previously described procedure, with some modifications (26, 27). Briefly, after treatment NCMs were rinsed in ice-cold PBS and collected in GTP-binding buffer (20 mM Tris-HCl pH 7.5, 5 mM $MgCl_2$, 2 mM PMSF, 150 mM NaCl, 0.1% Triton X-100, 0.025 mM PUGNAc and 1:1000 diluted protease and phosphase inhibitor mixture (Thermo Scientific)). Samples were sonicated for 15 s and centrifuged at 1,500 $\times$ *g* for 15 min at 4 °C, and the supernatant was collected. The protein concentration of each supernatant was determined by the Bradford assay. 200 μg protein were pre-cleared using the control agarose resin and then incubated with 100 μl of GTP-agarose beads (Sigma-Aldrich; equilibrated in GTP-binding buffer) in a total of 500 μl of GTP-binding buffer for 30 min at 4 °C. The beads were centrifuged at 10,000 $\times$ *g* for 2 min and the supernatant was retained. Then, the beads were washed three times with 1 ml of GTP-binding buffer and the retained supernatant was incubated with the beads for another 30 min. The beads were washed again as described above and then incu-

bated with the retained supernatant overnight at 4 °C. After washing seven times with GTP-binding buffer, bound protein was eluted from the beads by boiling them in 50 μl of 2x reducing SDS-PAGE buffer. DRP1 that was pulled-down by the GTP-agarose beads was quantified by Western blotting.

Detection of Glycosylated DRP1 with Wheat Germ Agglutinin-conjugated Beads—WGA-conjugated beads were used to precipitate the *O*-GlcNAcylated DRP1 as described previously (28). Hearts of control or diabetic mice were homogenized in lysis buffer (10 mM Tris (pH 7.4), 0.25 M mM sucrose, 3 mM $MgCl_2$, 1 mM β-glycerolphosphate, 2.5 mM Na-pyrophosphate, Na_3-VO_4, 10% glycerol, 0.025 mM PUGNAc, 1:1000 diluted protease and phosphase inhibitor mixture) using a Polytron homogenizer and centrifuged at 1500 × *g* for 15 min at 4 °C. Lysates were precleared using control agarose and incubated with WGA beads overnight. 200 μg of heart protein lysate in 200 μl of lysis buffer, as described above, were used in each reaction. After incubation, WGA-conjugated beads were centrifuged at 2300 × *g* for 5 min and resuspended with 2× SDS-PAGE buffer and analyzed by Western blot analysis.

Immunoprecipitation—Immunoprecipitation was performed using the Pierce Crosslink immunoprecipitation kit (Thermo Scientific) according to the instructions of the manufacturer. Briefly, 500 μg of total protein per immunoprecipitation reaction were used. To reduce nonspecific binding, the protein lysate was precleared using the control agarose resin. 10 μg of antibody was incubated with the A/G-plus agarose for 1 h at room temperature. After three washes, the precleared protein lysate was incubated with the A/G-plus agarose coupled with the antibody overnight at 4 °C. After four washes, the bound protein was eluated. The eluate was resolved by SDS-PAGE, and the gel was used for Western blotting.

Western Blotting—After treatment, cells were harvested using lysis buffer (20 mM Tris (pH 7.4), 20 mM NaCl, 0.1 mM EDTA, 0.025 mM PUGNAc, 1% Triton X-100, 1:1000 diluted protease, and phosphase inhibitor mixture). Samples were loaded on NuPAGE 4–12% Bis-Tris gels (Invitrogen). Separated proteins were transferred to PVDF membranes. The membranes were blocked in 5% nonfat milk. The membranes were immunoblotted with the following antibodies: anti-DRP1 (1:1000), anti-phosphorylated DRP1 (pDRP1, 1:1000), anti-porin (1:2000), and anti-*O*-GlcNAc [RL2] (1:1000). Anti-mouse (1:1000) and anti-rabbit (1:2000) HRP conjugates were used as secondary antibodies.

Identification of O-GlcNAc Sites by ETD MS/MS Analysis—Immunoprecipitated DRP1 from neonatal cardiomyocytes was used for the detection of *O*-GlcNAc sites. The detection and localization of serine and threonine residues modified with *O*-GlcNAc moiety was done on the basis of electron transfer dissociation (ETD) mass spectrometry technology, which fragments peptides by transferring an electron from a radical anion to a protonated peptide, resulting in peptide backbone fragmentation (29). ETD preserves modifications that are labile by traditional collision-induced dissociation, such as phosphorylation and glycosylation. Thus, sequence information on the peptide can be obtained.

The protein digests were pressure-loaded onto a 250-μm inside diameter (i.d.) fused silica capillary (Polymicro Technologies) column with a Kasil frit packed with 3 cm of 5-μm Partisphere-strong cation exchange resin (Whatman) and 3 cm of 5-μm C18 resin (Phenomenex). After desalting, this biphasic column was connected to a 100-μm i.d. fused silica capillary (Polymicro Technologies) analytical column with a 5-μm pulled tip, packed with 10 cm of 3-μm C18 resin (Phenomenex). The multidimensional protein identification technology (MudPIT) column was placed in line with an 1100 quaternary HPLC pump (Agilent Technologies), and the eluted peptides were electrosprayed directly into an LTQ Orbitrap XL mass spectrometer (Thermo Scientific). The buffer solutions used were 5% acetonitrile/0.1% formic acid (buffer A), 80% acetonitrile/0.1% formic acid (buffer B), and 500 mM ammonium acetate/5% acetonitrile/0.1% formic acid (buffer C). An 11-step MudPIT was run with salt pulses of 0%, 10%, 20%, 30%, 40%, 50%, 60%, 70%, and 100% buffer C; 90% buffer C/10% buffer B; and 80% buffer C/20% buffer B. The 120-min elution gradient had the following profile: 15% buffer B at 12.5 min, to 45% buffer B at 90 min, to 75% buffer B at 100 min, to 100% buffer B from 101–110 min. A cycle consisted of one full scan mass spectrum (300–1200 *m*/*z*) followed by eight data-dependent ETD MS/MS spectra with an isolation width of 3 *m*/*z*. Fluoranthene anions were set to a target value of 3e5, and ETD reaction time was set at 100 ms. Supplemental activation was enabled. Dynamic exclusion and early expiration were enabled. Application of mass spectrometer scan functions and HPLC solvent gradients were controlled by the Xcalibur data system (Thermo Scientific). ETD MS/MS spectra were extracted using RawXtract (version 1.9.9) (30). ETD MS/MS spectra were searched with the ProLuCID algorithm (31) against a rat UniProt database concatenated to a decoy database in which the sequence for each entry in the original database was reversed (32). Charged reduced precursors were removed from the spectra prior to searching. The ProLuCID search was performed using no enzyme specificity. Differential modifications considered were serine or threonine *O*-GlcNAcylation (203.0794). ProLuCID search results were assembled and filtered using the DTASelect (version 2.0) algorithm (33) with a false positive rate below 1%.

Mitochondrial Membrane Potential Measurement—The mitochondrial membrane potential was measured by JC-1, as described previously (24). NCMs were loaded with 0.5 mM JC-1 at 37 °C for 15 min and washed three times with media. The cells were visualized under a Nikon Diaphot epifluorescence microscope equipped with a ×40 fluor objective interfaced to a Photon Technologies, Inc. dual emission system, with the excitation wavelength set to 485 nm via a monocromator. Fluorescence emission was split and directed to two photomultiplier tubes through 20-nm band-pass filters centered at 531 and 584 nm, respectively. In addition, an aperture mechanism allowed fluorescence to be collected from a selected area, which was always positioned over the cytoplasmic region of individual cells. Data were shown as a ratio (F_{584}/F_{531}). Loss of mitochondrial membrane potential is indicated by a decrease in the red (F_{584})/green (F_{531}) fluorescence intensity ratio.

Mitochondrial Fragmentation—After treatment, mitochondrial morphology was observed. Cells were stained with 10^{-7} M MitoTracker Green FM for 30 min to visualize mitochondrial

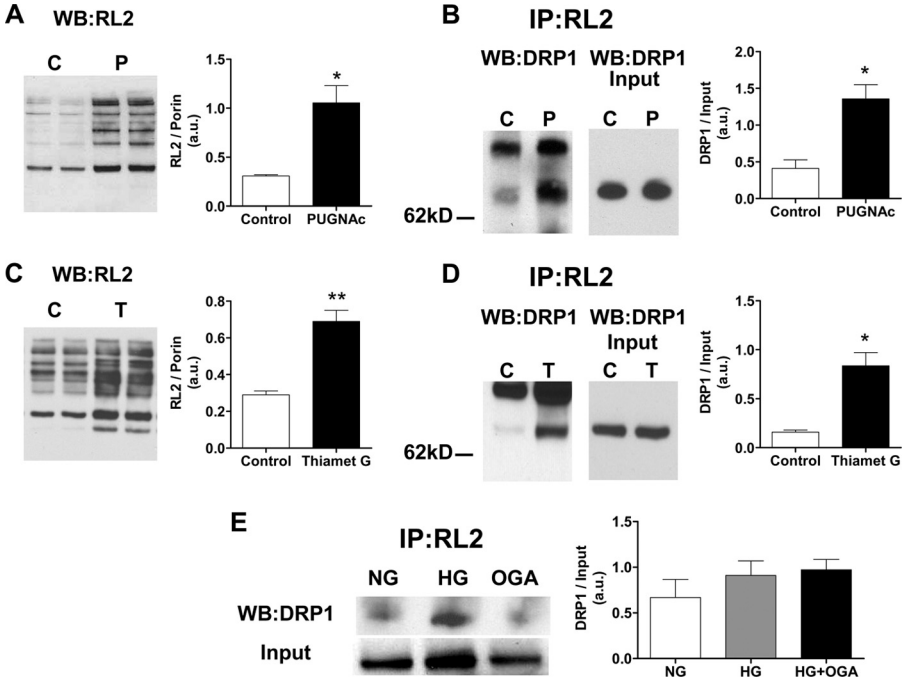

FIGURE 1. **DRP1 is modified by *O*-GlcNAcylation.** NCMs were treated with 100 μM PUGNAc (*P*) or 100 nM Thiamet G or with an equal volume of ethanol (the solvent used for PUGNAc and Thiamet G) as control for 24 h. *A* and *C*, whole cell lysates from NCMs treated with PUGNAc (*A*) or Thiamet G (*C*) were separated and analyzed by Western blot analysis (*WB*). The membrane was probed with anti-*O*-GlcNAc antibody (*RL2*). *B* and *D*, *O*-GlcNAcylated proteins were immunoprecipitated (*IP*) from whole cell lysates with RL2. The membrane was immunoblotted with anti-DRP1 antibody. *Input* represents DRP1 in NCM whole lysate used for immunoprecipitation. *E*, NCMs were infected by Adv-control or Adv-OGA (*OGA*) for 24 h. Cells were washed and treated with NG (5 mM) or HG (25 mM) for 72 h. *O*-GlcNAcylated proteins were immunoprecipitated from whole cell lysates with RL2. The membrane was immunoblotted with anti-DRP1 antibody. Graphs show densitometry values of protein *O*-GlcNAcylation. Signals were normalized with porin or input, as indicated. $n = 3$; *, $p < 0.05$ *versus* control; **, $p < 0.01$ *versus* control. Data are expressed as means ± S.E. C = control. *p*, PUGNAc, *T* = Thiamet G.

morphology and then washed three times with media. Images were captured with a DeltaVision deconvolution microscope system (Applied Precision) located at the University of California, San Diego Cancer Center microscope facility. Using a ×60 (numerical aperture 1.4) lens, images of ~50 serial optical sections, spaced by 0.2 μm, were acquired. The data sets were deconvolved using SoftWorx software (Applied Precision) on a Silicon Graphics Octane work station. Because cardiomyocytes have two different types of mitochondrial structure (center, round; pseudopod area, tubular) and we observed morphological change only in the pseudopod area, we eliminated the center area and analyzed only the pseudopod area where the thickness is less than 0.6 μm. The morphological changes are described using the parameter of roundness ((perimeter length)^2/(4 × π × area)) using ImagePro-PLUS software (Media Cybernetics, Inc.).

Statistics—Results of the experimental studies are reported as mean ± S.E. Differences were analyzed by Student's *t* test or one-way analysis of variance followed by Newman-Keuls multiple comparison post-test using GraphPad Prism version 5.02 for Windows (GraphPad Software). $p < 0.05$ was regarded as statistically significant.

RESULTS

DRP1 Is O-GlcNAcylated in Rat Neonatal Cardiac Myocytes—We used the well known OGA inhibitor PUGNAc to increase overall *O*-GlcNAc levels in cell culture. The novel OGA inhibitor Thiamet G was also used in some experiments to rule out off target effects. Western blot analysis with whole cell lysates using the *O*-GlcNAc (RL2) antibody determined that treatment of NCMs with the OGA inhibitors PUGNAc and Thiamet G results in increased *O*-GlcNAc modification of proteins (Fig. 1). To determine DRP1-specific *O*-GlcNAcylation, we used an approach that was used recently with inositol triphosphate receptor 3 (34). *O*-GlcNAc proteins were immunoprecipitated from whole cell lysate using an anti-O-GlcNAc antibody RL2, followed by SDS-PAGE and Western blotting with anti-DRP1. As shown in Fig. 1*B*, there is a basal *O*-GlcNAcylation of DRP1. Inhibition of OGA by PUGNAc resulted in increased *O*-GlcNAc modification. As shown in Fig. 1*D*, Thiamet G treatment also resulted in increased *O*-GlcNAc modification of DRP1. High-glucose treatment resulted in a more intense *O*-GlcNAc DRP1 Western blot band. However, because high glucose also induces increased DRP1 expression, the ratio of the immunoprecipitation band to the input band is not significantly different from the control.

Localization of O-GlcNAc sites in DRP1—Analysis of DRP1 by ETD MS/MS demonstrated that the residues Thr-585 and Thr-586 are *O*-GlcNAcylated (Fig. 2*A*). DRP1 is composed of GTP-binding (Fig. 2*B*, *middle, insert B*) and GTPase effector domains. The two identified *O*-GlcNAc-modified residues are located in the insert B domain (Fig. 2*B*).

Increase of O-GlcNAcylation Decreases Phosphorylation of DRP1 at Ser-637—DRP1 is regulated by phosphorylation at specific Ser residues. As it is known that phosphorylation and *O*-GlcNAcylation both modify Ser residues and that these two reactions are competitive, we determined whether increased

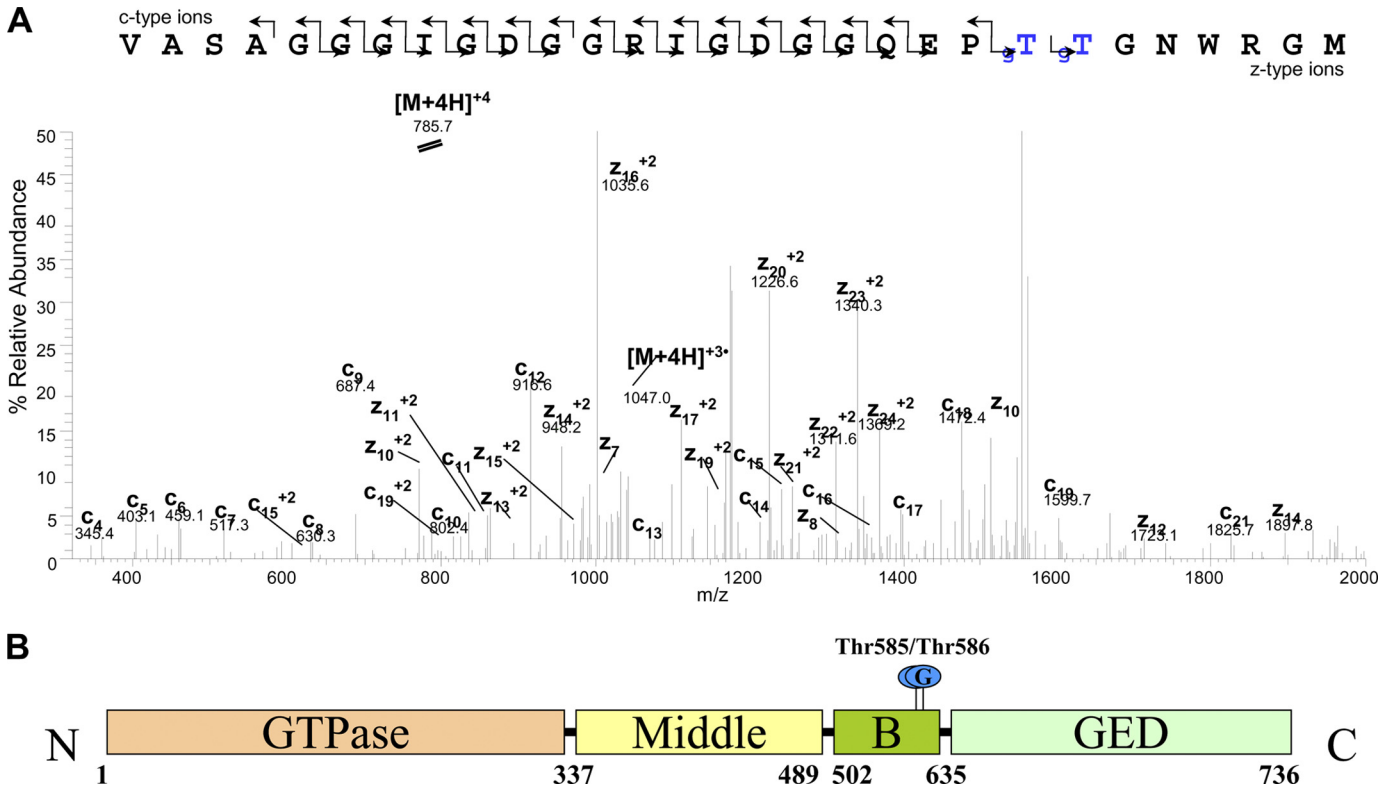

FIGURE 2. ***O*-GlcNAc site mapping on DRP1.** *A*, ETD MS/MS spectrum of [M+4H] +4 ion. *B*, schematic diagram showing the identified *O*-GlcNAc sites Thr-585 and Thr-586 within the B domain of DRP1.

O-GlcNAcylation has an impact on DRP1 phosphorylation. In cells treated with PUGNAc or Thiamet G, there was a significant decrease of Ser-637 phosphorylation as determined by Western blotting (control, 1.1 ± 0.06 a.u.; PUGNAc, 0.8 ± 0.05 a.u.; $p < 0.001$ and control, 0.97 ± 0.04 a.u.; Thiamet G, 0.4 ± 0.05 a.u.; $p < 0.001$) (Fig. 3, *A* and *B*). Increased *O*-GlcNAcylation had no effect on the expression of DRP1 (Fig. 3, *A* and *B*). Because our previous studies showed that high glucose treatment, which increases *O*-GlcNAcylation, increases mitochondrial fragmentation (24), NCMs were treated with high glucose for 72 h to investigate the impact of high glucose on phosphorylation of DRP1. To parse the effects of high glucose treatment from the effects of increased *O*-GlcNAcylation, high glucose-treated cells were also infected with Adv-OGA to overexpress OGA and decrease high glucose-induced enhanced *O*-GlcNAcylation in these cells. In our previous work, we have shown that high glucose treatment increases the overall *O*-GlcNAcylation of proteins and that infection with Adv-OGA results in overexpression of OGA and subsequently diminishes the high glucose-induced *O*-GlcNAcylation. As shown in Fig. 3*C*, high glucose increases the expression of DRP1. However, OGA overexpression does not return the high glucose-induced increase of DRP1, indicating that this increase is *O*-GlcNAcylation-independent (NG, 0.62 ± 0.06 a.u.; HG, 0.99 ± 0.07 a.u.; HG+OGA, 0.88 ± 0.08 a.u.; $p < 0.05$ *versus* NG). In addition, high glucose decreases the phosphorylation of Ser-637 in DRP1. However, OGA overexpression improves this reduction only slightly and not significantly (NG, 1.09 ± 0.09 a.u.; HG, 0.53 ± 0.09 a.u.; HG+OGA, 0.77 ± 0.12 a.u.; $p < 0.05$ *versus* NG). Neither the OGA inhibitors nor high glucose had an impact on the Ser-616 phosphorylation.

O-GlcNAcylation Affects the GTP-binding Properties of DRP1—GTP binding induces conformational changes of DRP1, which in turn are functionally critical for DRP1-induced mitochondrial fission (35). To investigate if *O*-GlcNAcylation affects the GTP-binding properties of DRP1, NCMs were treated with PUGNAc or Thiamet G or high glucose with or without Adv-OGA. The cell lysates were subjected to a pull-down assay using GTP beads. As shown in Fig. 4, inhibition of OGA by PUGNAc or Thiamet G resulted in increased DRP1 GTP-binding activity (control, 0.51 ± 0.07; PUGNAc, 1.03 ± 0.09; $p < 0.01$ and control, 0.74 ± 0.03; Thiamet G, 1.07 ± 0.1; $p < 0.05$). High glucose treatment also resulted in increased GTP-binding, which was normalized by the overexpression of OGA (NG, 0.43 ± 0.04; HG, 0.58 ± 0.03; HG+OGA, 0.40 ± 0.06; $p < 0.05$) (Fig. 4*B*). These results show clearly that *O*-GlcNAcylation modifies the GTP-binding affinity of DRP1.

O-GlcNAcylation Influences the Distribution of DRP1—The majority of DRP1 proteins are localized in the cytoplasm. However, dephosphorylation induces the translocation of DRP1 from cytoplasm to mitochondria (7). Accordingly, we analyzed if *O*-GlcNAcylation also affects distribution of DRP1. FIS1 is a mitochondrial outer membrane protein that tethers DRP1 to mitochondria (15, 36). Using a FIS1 antibody to identify mitochondria, we have shown that the majority of DRP1 in untreated cells is localized in the cytoplasm (Fig. 5). For both PUGNAc and high glucose treatment, we performed a Western blot analysis to determine the DRP1 distribution. Fig. 5 shows that increasing *O*-GlcNAcylation by PUGNAc or high glucose

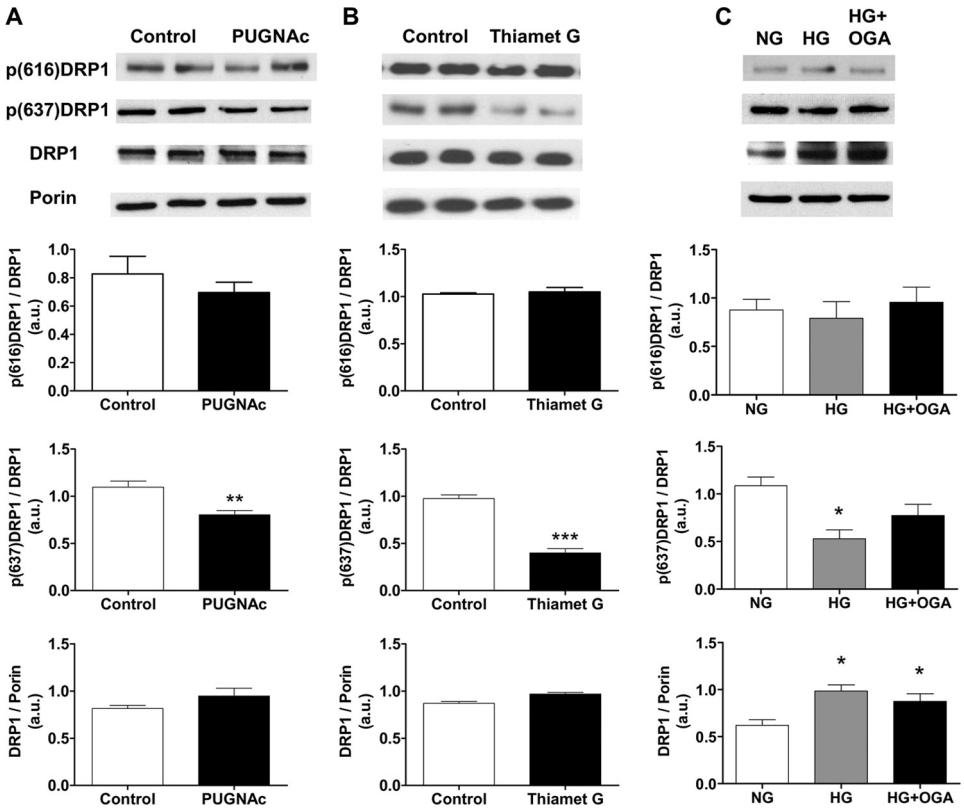

FIGURE 3. ***O*-GlcNAcylation decreases phosphorylation of p(637)DRP1.** *A* and *B*, NCMs were exposed to PUGNAc (100 μM) or Thiamet G (100 nM) or control (solvent only) for 24 h. DRP1 and phospho-DRP1 levels were determined by Western blot analysis. Representative Western blot analyses are shown. Protein loading was normalized using an anti-porin antibody. Densitometric analysis for normalized DRP1 expression and phosphorylation levels are shown. $n = 3$–5; **, $p < 0.01$ *versus* control. Data are expressed as mean ± S.E. *C*, NCMs were infected by Adv-control or Adv-OGA (*OGA*) for 24 h. Cells were washed and treated with NG (5 mM) or HG (25 mM) for 72 h. Western blot analysis was performed with anti-DRP1, anti-phospho-(616)DRP1, anti-phospho-(637)DRP1, and anti-porin antibodies. Graphs of normalized densitometric analysis for DRP1 expression or phosphorylation levels are shown. $n = 3$–4; *, $p < 0.05$ *versus* NG. Data are expressed as mean ± S.E.

treatment results in translocation of DRP1 from cytoplasm to mitochondria. OGA overexpression restores the high glucose-induced translocation.

PUGNAc Treatment Increases Mitochondrial Fragmentation and Decreases Mitochondrial Membrane Potential—In our previous work we showed that high glucose treatment increases mitochondrial fragmentation and decreases mitochondrial membrane potential and that OGA overexpression returned the values close to the level of control (24). In this study, we analyzed the impact of the OGA inhibitor PUGNAc on these mitochondrial changes. As shown in Fig. 6, *A* and *B*, PUGNAc significantly increases mitochondrial fragmentation (mean roundness, control 5.10 ± 0.25; PUGNAc 4.34 ± 0.141; $p < 0.01$). PUGNAc also induces significant mitochondrial depolarization (membrane potential, control 2.97 ± 0.16; PUGNAc 1.82 ± 0.14; $p < 0.001$) (Fig. 6*C*), confirming the suggestion that excessive *O*-GlcNAcylation decreases mitochondrial membrane potential and increases mitochondrial fragmentation.

Cardiac DRP1 Is Significantly More O-GlcNAcylated in Type 2 Diabetic Mice—WGA binds to GlcNAc residues, and WGA-conjugated agarose beads bind to *O*-GlcNAc-modified proteins with high affinity. We used WGA-conjugated agarose beads to determine whether DRP1 from type 2 diabetic mice is more glycosylated compared with control mice. As shown in Fig. 7, DRP1 is significantly more glycosylated in diabetic hearts (control, 0.42 ± 0.01 a.u.; 0.84 ± 0.1 a.u.; $p < 0.05$). In addition, *O*-GlcNAc cardiac proteins were immunoprecipitated from whole heart lysate using the anti-*O*-GlcNAc antibody RL2 followed by SDS-PAGE and Western blotting with anti-DRP1. DRP1 from type 2 diabetic mice appeared to be more *O*-GlcNAcylated (control, 0.74 ± 0.03 a.u.; 1.15 ± 0.9 a.u.; $p < 0.05$). Because the antibody for phospho-637-DRP1 does not bind the mouse DRP1 and there are no alternative antibodies available, we were not able to determine the phosphorylation of this site. There was no difference between diabetes and control regarding the phosphorylation of Ser-616 of DRP1.

DISCUSSION

In this study we show that DRP1 is modified by *O*-GlcNAcylation in cardiomyocytes and that DRP1 phosphorylation, which regulates DRP1-dependent mitochondrial fission, is affected by the level of *O*-GlcNAcylation. We treated cardiomyocytes with PUGNAc or Thiamet G, which inhibit OGA. OGA removes *O*-GlcNAcylation from serine and threonine residues, so inhibition of OGA results in increased *O*-GlcNAcylation, as shown in Fig. 1, *A* and *C*. To analyze if DRP1 is modified by *O*-GlcNAcylation, we immunoprecipitated NCMs lysates with the antibody anti-*O*-GlcNAc, and performed a Western blot analysis for DRP1. As shown in Fig. 1, *B* and *D*, we found a basal *O*-GlcNAcylation in cardiac DRP1 and inhibition of OGA increased the DRP1 modification. There are also other possible strategies for increasing or preventing *O*-GlcNA-

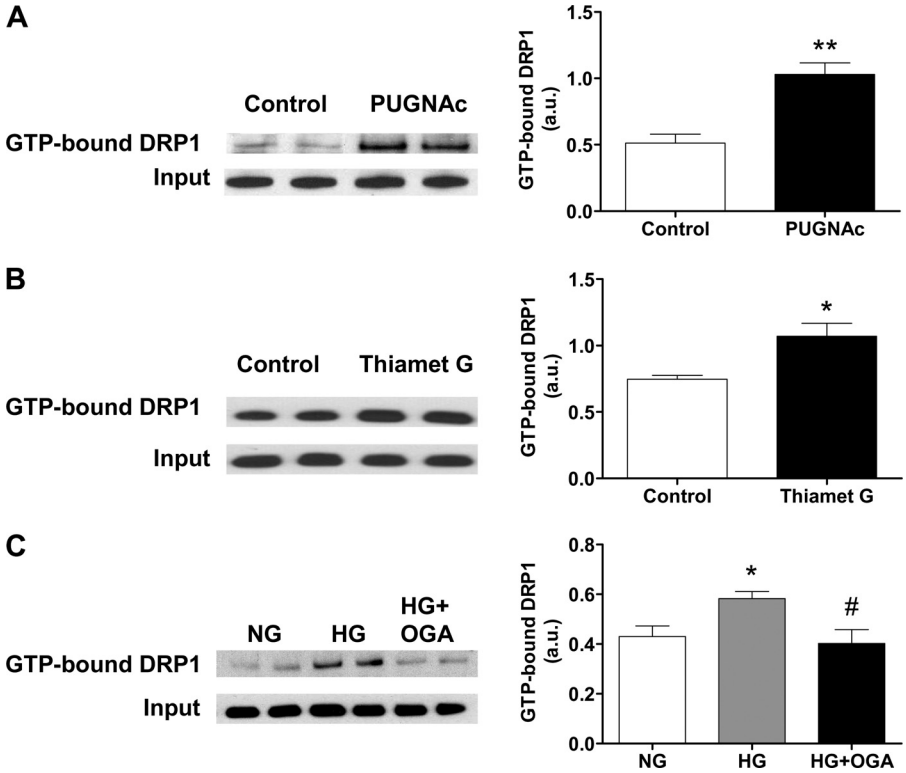

FIGURE 4. ***O*-GlcNAcylation increases DRP1 GTP-binding.** *A* and *B*, PUGNAc (100 μM) or Thiamet G (100 nM) or control-treated NCMs were collected using GTP-binding buffer. 200 μl of protein lysate was incubated with GTP-agarose beads. After several washing steps, bound protein was eluted from the beads. DRP1 that had bound to the GTP-agarose beads was visualized by Western blotting. Representative Western blot analyses are shown. Values were normalized to DRP1 levels in lysate used for the pull-down of GTP-binding proteins (*input*). $n = 4$; *, $p < 0.05$ *versus* control; **, $p < 0.01$ *versus* control. Data are expressed as mean ± S.E. *C*, NCMs were infected by Adv-control or Adv-OGA (*OGA*) for 24 h. Cells were washed and treated with NG (5 mM) or HG (25 mM) for 72 h. NCM lysates were used for a GTP pull-down assay. $n = 4$; *, $p < 0.05$ *versus* NG; #, $p < 0.05$ *versus* HG. Data are expressed as mean ± S.E.

cylation. In further studies, the impact on DRP1 function of increasing *O*-GlcNAc modification by *N*-acetylglucosamine treatment combined with OGT RNA silencing should be also investigated.

Others reported several post-translational modifications of DRP1, like phosphorylation (5–7), SUMOylation (8), ubiquitination (9), and *S*-nitrosylation (10). Here we show for the first time that *O*-GlcNAcylation is an additional type of modification occurring in DRP1. Because *O*-GlcNAcylation can affect the phosphorylation of proteins even if they are located at different domains (19, 37, 38), we analyzed if increasing *O*-GlcNAcylation affects the level of the two known phosphorylation sites of DRP1, Ser-616 and Ser-637. In cells treated with PUGNAc or Thiamet G, we have seen decreased phosphorylation at Ser-637. The phosphorylation at Ser-616 was not affected. Because high glucose treatment also results in increased *O*-GlcNAcylation, we investigated whether high glucose treatment has a similar effect on phosphorylation of DRP1. As shown in Fig. 3, high glucose had no effect on Ser-616 but causes a decrease in Ser-637 phosphorylation. However, OGA overexpression does not return the value to normal. There is only a slight, non-significant increase in phosphorylation. Why OGA does not return the high glucose-induced decrease of Ser-637 phosphorylation to normal although inhibition of OGA by PUGNAc decreases the phosphorylation is a matter for speculation. Ser-637 is phosphorylated by cAMP-dependent protein kinase and several reports described a stimulating impact of high glucose on the activity of cAMP-dependent protein kinase in different cell types (39–41). In the case of DRP1, the balance between the influence of high glucose on cAMP-dependent protein kinase activity and the impact of increased *O*-GlcNAcylation can be of importance. It is possible that increased *O*-GlcNAcylation directly affects the activity of cAMP-dependent protein kinase and/or calcineurin, which dephosphorylates DRP1. It is also possible that *O*-GlcNAcylation of Ser-637 or other proximal residues affects the phosphorylation of Ser-637. Further studies are needed to investigate this interesting interplay in detail. In addition, high glucose increases the expression of DRP1 independently of *O*-GlcNAcylation (Fig. 3). Interestingly, in our previous work we have shown that treatment of NCMs with 35 mM glucose for 24 h decreases DRP1 levels (24). In this study, we demonstrate that treatment with 25 mM glucose for 72 h increases DRP1 levels. These results indicate that DRP1 expression is glucose-sensitive, which should be further investigated in future studies.

Chang and Blackstone (5) reported that phosphorylation of DRP1 at Ser-637 inhibits DRP1 GTPase activity. Because inhibition of OGA and high glucose treatment resulted in decreased Ser-637 phosphorylation, we examined if there is an impact on the GTP-binding affinity of DRP1. Our results show that both PUGNAc and Thiamet G as well as high glucose increase DRP1 GTP-binding and that OGA overexpression returns the high glucose-induced GTP-binding increase to normal. Considering the PUGNAc results only, it is not possible to

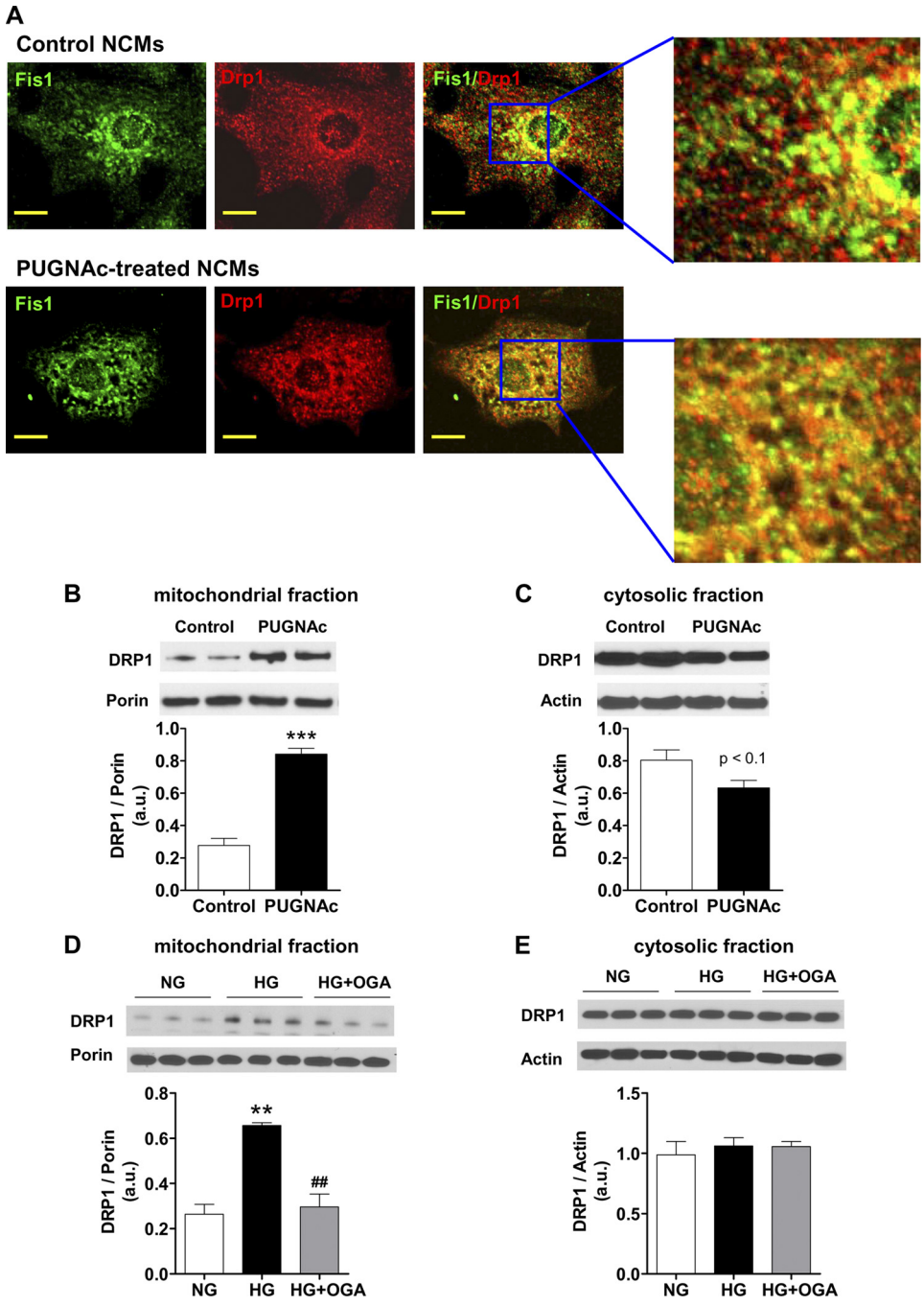

FIGURE 5. **Subcellular distribution of DRP1 in cultured cardiomyocytes.** *A*, control cells or cells treated with PUGNAc (100 μM) for 24 h were stained for DRP1 (*red*) and FIS1 (*green*) and analyzed by confocal microscopy. Images are representative of three independent determinations. *Scale bar* = 10 μm. *B* and *C*, subcellular fractions of NCMs were separated by SDS/PAGE and immunoblotted with the indicated antibodies. $n = 3$; ***, $p < 0.001$ *versus* control; **, $p < 0.01$ *versus* NG; ##, $p < 0.01$ *versus* HG. Data are expressed as mean ± S.E.

attribute the increase in the DRP1 GTP-binding affinity to the enhancement of *O*-GlcNAcylation alone. Because GTPase activity is dependent on phosphorylation, a PUGNAc-induced dephosphorylation should increase the GTP-binding affinity of DRP1. This would only allow the conclusion that *O*-GlcNAc-induced dephosphorylation increases the GTP-binding of DRP1. However, OGA overexpression had no effect on high glucose-induced phosphorylation (Fig. 3), but it did return the high glucose-induced increase of GTP-binding to normal (Fig. 4), indicating that *O*-GlcNAcylation increases GTP-binding affinity independent of phosphorylation. Our results demonstrate that increasing the overall *O*-GlcNAcylation affects the GTP-binding properties of DRP1. To understand the direct impact of *O*-GlcNAcylation on DRP1 GTPase activity in detail, a more comprehensive GTPase activity study is required. DRP1 harbors four distinct domains: GTP-binding, middle, insert B, and GTPase effector (42). Using ETD MS/MS we were able to detect the *O*-GlcNAc sites Thr-585 and Thr-586, located at the insert B domain of DRP1. The insert B domain contains several different posttranslational modifications that modulate DRP1

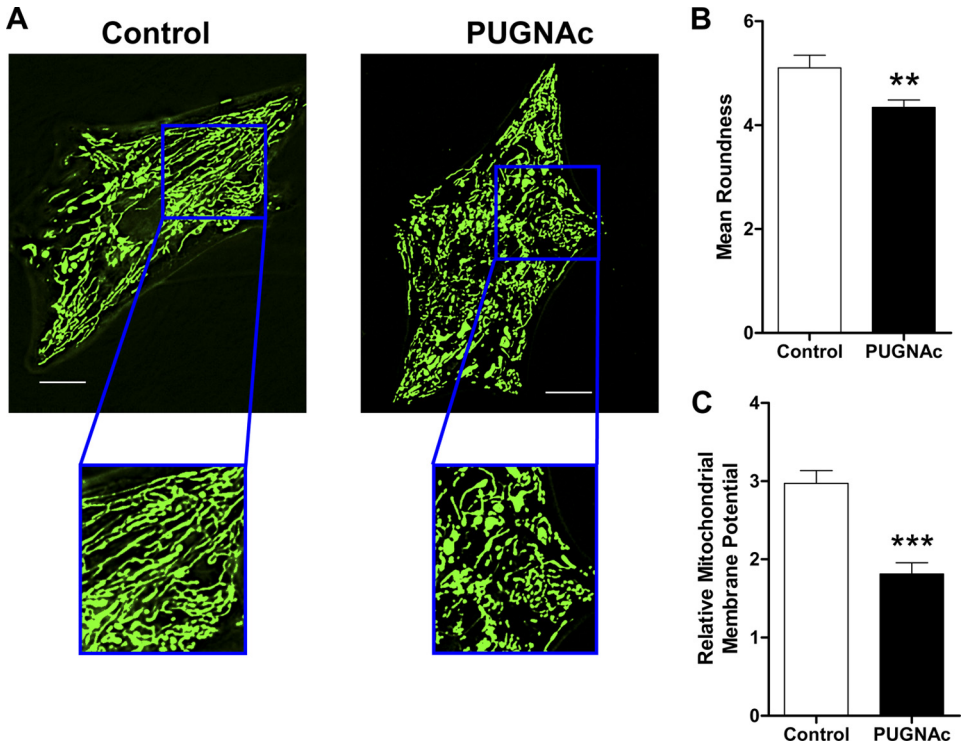

FIGURE 6. **PUGNAc induces mitochondrial fragmentation in NCMs and decreases mitochondrial membrane potential.** *A*, after treatment, cells were loaded with MitoTracker Green FM for mitochondrial staining. Representative images of mitochondrial morphology are shown. *B*, mitochondrial morphological change is analyzed by the mean roundness. $n = 10$ NCMs; **, $p < 0.001$ *versus* control. Data are expressed as mean ± S.E. *Scale bar* = 10 μm. *C*, cells were loaded with JC-1 for analysis of membrane potential. The graph shows relative mitochondrial membrane potential (red/green fluorescence ratio). $n = 30$ NCMs; ***, $p < 0.001$ *versus* control. Data are expressed as mean ± S.E.

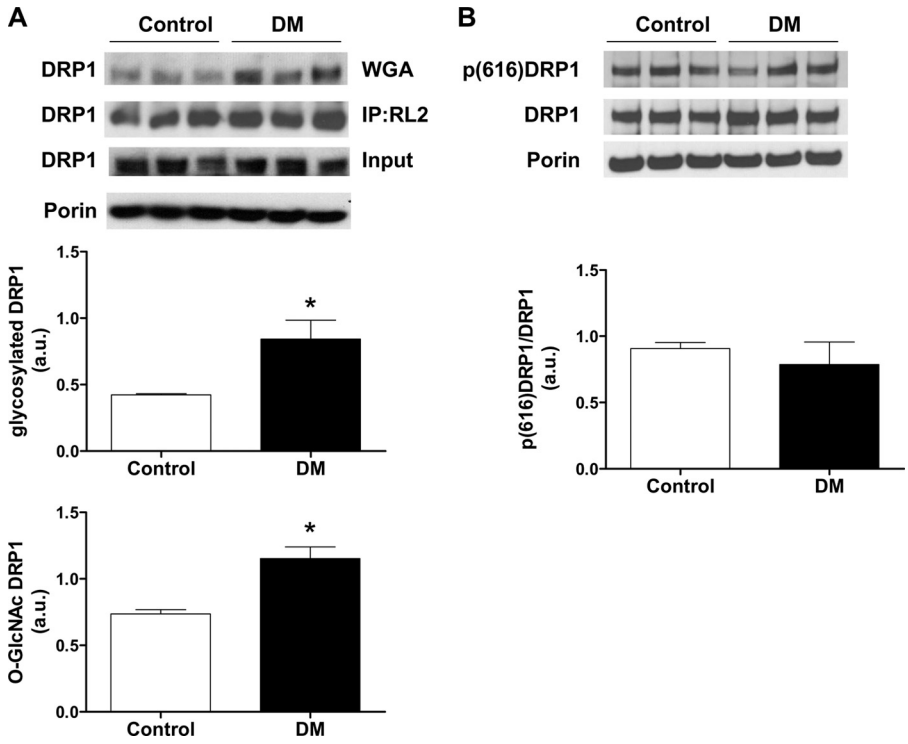

FIGURE 7. **Increased DRP1 *O*-GlcNac modification in type 2 diabetic mice.** *A*, lysates from whole hearts of control or diabetic mice were incubated with WGA-agarose beads overnight. After incubation, beads were centrifuged, and protein was resuspended with 2× Laemmli buffer and analyzed by Western blot analysis. *O*-GlcNAcylated proteins were immunoprecipitated from whole cell lysates with RL2. The membrane was immunoblotted with anti-DRP1 antibody. $n = 3$; *, $p < 0.05$ *versus* control. Data are expressed as mean ± S.E. *B*, Western blot analysis was performed with anti-DRP1, anti-phospho-(616)DRP1, and anti-porin antibodies. Graphs of normalized densitometric analysis for DRP1 expression or phosphorylation levels are shown. Data are expressed as mean ± S.E.

function, including phosphorylation and SUMOylation. *O*-GlcNAcylation of the two threonine residues within this domain could have an impact on the oligomerization of DRP1 monomers or the interaction with other proteins. Using ETD MS/MS we were able to identify the *O*-GlcNAc sites Thr-585 and Thr-586. However, we cannot rule out the existence of additional *O*-GlcNAc sites in DRP1, including Ser-616 and Ser-637. Further investigation is needed on this matter.

In addition to GTPase activity and protein expression, DRP1 function can also be affected by processes such as mitochondrial translocation or protein interactions. DRP1 recruitment to mitochondria is increased prominently during events such as programmed cell death (43). The key event in DRP1 regulation occurs at the mitochondrial recruitment step. Here we show that increasing overall *O*-GlcNAcylation in cardiomyocytes results in recruitment of DRP1 from cytoplasm to mitochondria. FIS1 is a mitochondrial outer membrane protein, which has been reported to interact with DRP1, resulting in increased mitochondrial fragmentation (13, 15). Otera *et al.* (14) have reported that mitochondrial fission factor is responsible for DRP1 recruitment to the mitochondrial outer membrane (14). In this study, we did not investigate the impact of *O*-GlcNAcylation on the interaction of DRP1 with FIS1 or mitochondrial fission factor. Here we show that increasing *O*-GlcNAcylation results in recruitment of DRP1 to the mitochondria by showing colocalization of DRP1 with FIS1 (Fig. 5) and by Western blot analysis using mitochondrial and cytosolic fractions.

As shown in Fig. 6, increasing overall *O*-GlcNAcylation by PUGNAc treatment results in mitochondrial fragmentation and decreased mitochondrial membrane potential. In our previous work we have shown that high glucose-induced *O*-GlcNAcylation affects mitochondrial fragmentation and membrane potential, an effect which was attributed to increased *O*-GlcNAcylation of the mitochondrial fusion protein OPA1 (24). Here we show with DRP1 that another key player in the mitochondrial fusion/fission process is modified by *O*-GlcNAcylation and that increased global modification modulates its function. Interestingly, increased *O*-GlcNAcylation seems to inhibit OPA1 activity (24). However, in the case of DRP1, protein activity is enhanced by increased *O*-GlcNAcylation.

Taken together, our data demonstrate that DRP1 is *O*-GlcNAcylated and that alteration of the level of global *O*-GlcNAcylation alters DRP1 function. Increasing *O*-GlcNAcylation results in enhanced DRP1 GTP-binding ability and recruitment of DRP1 to mitochondria. The resulting effect on mitochondrial function is likely not just an impact of the increased *O*-GlcNAcylation of DRP1. Gu *et al.* (44) already reported *O*-GlcNAc modification of several mitochondrial proteins, including prohibitin and HSP60. Modification of other fusion/fission proteins could also affect mitochondrial morphology and function. However, because the overall *O*-GlcNAc modification of cytosolic proteins is much higher than that of mitochondrial proteins (18), modulation of DRP1 function (which is a cytosolic protein) by *O*-GlcNAcylation is likely to have a key role in mitochondrial function. It should also be mentioned that a high glucose-mediated, sustained increase in *O*-GlcNAcylation has been linked to the development of diabetes-related cardiovascular complications (45, 46). Mitochondrial dysfunction in diabetic cardiomyocytes is also well known (47). However, the underlying mechanisms have not been completely explained. In our previous study we showed increased *O*-GlcNAcylation of mitochondrial proteins in cultured cardiomyocytes exposed to high glucose (18). In this report we show increased *O*-GlcNAcylation of cardiac DRP1 in type 2 diabetic mice (Fig. 7). Furthermore, our *in vitro* results demonstrate that increased overall *O*-GlcNAcylation affects DRP1 functionality, resulting in impaired mitochondrial function. Altogether, these results imply that the impact of excessive overall *O*-GlcNAcylation on DRP1 function could play a significant role in the development of diabetic mitochondrial dysfunction.

REFERENCES

1. Westermann, B. (2010) Mitochondrial fusion and fission in cell life and death. *Nat. Rev. Mol. Cell Biol.* **11,** 872–884
2. Kane, L. A., and Youle, R. J. (2010) Mitochondrial fission and fusion and their roles in the heart. *J. Mol. Med.* **88,** 971–979
3. Chang, C. R., and Blackstone, C. (2010) Dynamic regulation of mitochondrial fission through modification of the dynamin-related protein Drp1. *Ann. N.Y. Acad. Sci.* **1201,** 34–39
4. Smirnova, E., Griparic, L., Shurland, D. L., and van der Bliek, A. M. (2001) Dynamin-related protein Drp1 is required for mitochondrial division in mammalian cells. *Mol. Biol. Cell* **12,** 2245–2256
5. Chang, C. R., and Blackstone, C. (2007) Cyclic AMP-dependent protein kinase phosphorylation of Drp1 regulates its GTPase activity and mitochondrial morphology. *J. Biol. Chem.* **282,** 21583–21587
6. Cribbs, J. T., and Strack, S. (2007) Reversible phosphorylation of Drp1 by cyclic AMP-dependent protein kinase and calcineurin regulates mitochondrial fission and cell death. *EMBO Rep.* **8,** 939–944
7. Cereghetti, G. M., Stangherlin, A., Martins de Brito, O., Chang, C. R., Blackstone, C., Bernardi, P., and Scorrano, L. (2008) Dephosphorylation by calcineurin regulates translocation of Drp1 to mitochondria. *Proc. Natl. Acad. Sci. U.S.A.* **105,** 15803–15808
8. Figueroa-Romero, C., Iñiguez-Lluhi, J. A., Stadler, J., Chang, C. R., Arnoult, D., Keller, P. J., Hong, Y., Blackstone, C., and Feldman, E. L. (2009) SUMOylation of the mitochondrial fission protein Drp1 occurs at multiple nonconsensus sites within the B domain and is linked to its activity cycle. *FASEB J.* **23,** 3917–3927
9. Nakamura, N., Kimura, Y., Tokuda, M., Honda, S., and Hirose, S. (2006) MARCH-V is a novel mitofusin 2- and Drp1-binding protein able to change mitochondrial morphology. *EMBO Rep.* **7,** 1019–1022
10. Cho, D. H., Nakamura, T., Fang, J., Cieplak, P., Godzik, A., Gu, Z., and Lipton, S. A. (2009) *S*-nitrosylation of Drp1 mediates β-amyloid-related mitochondrial fission and neuronal injury. *Science* **324,** 102–105
11. Jahani-Asl, A., and Slack, R. S. (2007) The phosphorylation state of Drp1 determines cell fate. *EMBO Rep.* **8,** 912–913
12. Taguchi, N., Ishihara, N., Jofuku, A., Oka, T., and Mihara, K. (2007) Mitotic phosphorylation of dynamin-related GTPase Drp1 participates in mitochondrial fission. *J. Biol. Chem.* **282,** 11521–11529
13. Stojanovski, D., Koutsopoulos, O. S., Okamoto, K., and Ryan, M. T. (2004) Levels of human Fis1 at the mitochondrial outer membrane regulate mitochondrial morphology. *J. Cell Sci.* **117,** 1201–1210
14. Otera, H., Wang, C., Cleland, M. M., Setoguchi, K., Yokota, S., Youle, R. J., and Mihara, K. (2010) Mff is an essential factor for mitochondrial recruitment of Drp1 during mitochondrial fission in mammalian cells. *J. Cell Biol.* **191,** 1141–1158
15. Yu, T., Fox, R. J., Burwell, L. S., and Yoon, Y. (2005) Regulation of mitochondrial fission and apoptosis by the mitochondrial outer membrane protein hFis1. *J. Cell Sci.* **118,** 4141–4151
16. Hart, G. W., Housley, M. P., and Slawson, C. (2007) Cycling of *O*-linked β-N-acetylglucosamine on nucleocytoplasmic proteins. *Nature* **446,** 1017–1022

17. Gewinner, C., Hart, G., Zachara, N., Cole, R., Beisenherz-Huss, C., and Groner, B. (2004) The coactivator of transcription CREB-binding protein interacts preferentially with the glycosylated form of Stat5. *J. Biol. Chem.* **279,** 3563–3572
18. Hu, Y., Suarez, J., Fricovsky, E., Wang, H., Scott, B. T., Trauger, S. A., Han, W., Hu, Y., Oyeleye, M. O., and Dillmann, W. H. (2009) Increased enzymatic *O*-GlcNAcylation of mitochondrial proteins impairs mitochondrial function in cardiac myocytes exposed to high glucose. *J. Biol. Chem.* **284,** 547–555
19. Cheng, X., and Hart, G. W. (2001) Alternative *O*-glycosylation/*O*-phosphorylation of serine-16 in murine estrogen receptor beta: post-translational regulation of turnover and transactivation activity. *J. Biol. Chem.* **276,** 10570–10575
20. Love, D. C., Kochan, J., Cathey, R. L., Shin, S. H., and Hanover, J. A. (2003) Mitochondrial and nucleocytoplasmic targeting of *O*-linked GlcNAc transferase. *J. Cell Sci.* **116,** 647–654
21. Clark, R. J., McDonough, P. M., Swanson, E., Trost, S. U., Suzuki, M., Fukuda, M., and Dillmann, W. H. (2003) Diabetes and the accompanying hyperglycemia impairs cardiomyocyte calcium cycling through increased nuclear *O*-GlcNAcylation. *J. Biol. Chem.* **278,** 44230–44237
22. Hu, Y., Belke, D., Suarez, J., Swanson, E., Clark, R., Hoshijima, M., and Dillmann, W. H. (2005) Adenovirus-mediated overexpression of *O*-GlcNAcase improves contractile function in the diabetic heart. *Circ. Res.* **96,** 1006–1013
23. Laczy, B., Hill, B. G., Wang, K., Paterson, A. J., White, C. R., Xing, D., Chen, Y. F., Darley-Usmar, V., Oparil, S., and Chatham, J. C. (2009) Protein *O*-GlcNAcylation. A new signaling paradigm for the cardiovascular system. *Am. J. Physiol. Heart Circ. Physiol.* **296,** H13–28
24. Makino, A., Suarez, J., Gawlowski, T., Han, W., Wang, H., Scott, B. T., and Dillmann, W. H. (2011) Regulation of mitochondrial morphology and function by O-GlcNAcylation in neonatal cardiac myocytes. *Am. J. Physiol. Regul. Integr. Comp. Physiol.* **300,** R1296–R1302
25. Gao, Y., Wells, L., Comer, F. I., Parker, G. J., and Hart, G. W. (2001) Dynamic *O*-glycosylation of nuclear and cytosolic proteins: cloning and characterization of a neutral, cytosolic β-*N*-acetylglucosaminidase from human brain. *J. Biol. Chem.* **276,** 9838–9845
26. Gundemir, S., and Johnson, G. V. (2009) Intracellular localization and conformational state of transglutaminase 2. Implications for cell death. *PLoS ONE* **4,** e6123
27. Zhao, J., Liu, T., Jin, S., Wang, X., Qu, M., Uhlen, P., Tomilin, N., Shupliakov, O., Lendahl, U., and Nister, M. (2011) Human MIEF1 recruits Drp1 to mitochondrial outer membranes and promotes mitochondrial fusion rather than fission. *EMBO J.* **30,** 2762–2778
28. Gandy, J. C., Rountree, A. E., and Bijur, G. N. (2006) Akt1 is dynamically modified with *O*-GlcNAc following treatments with PUGNAc and insulin-like growth factor-1. *FEBS Lett.* **580,** 3051–3058
29. Schroeder, M. J., Webb, D. J., Shabanowitz, J., Horwitz, A. F., and Hunt, D. F. (2005) Methods for the detection of paxillin post-translational modifications and interacting proteins by mass spectrometry. *J. Proteome Res.* **4,** 1832–1841
30. McDonald, W. H., Tabb, D. L., Sadygov, R. G., MacCoss, M. J., Venable, J., Graumann, J., Johnson, J. R., Cociorva, D., and Yates, J. R., 3rd. (2004) MS1, MS2, and SQT-three unified, compact, and easily parsed file formats for the storage of shotgun proteomic spectra and identifications. *Rapid Commun. Mass Spectrom.* **18,** 2162–2168
31. Xu, T., Venable, J. D., Park, S. K., Cociorva, D., Lu, B., Liao, L., Wohlschlegel, J., Hewel, J., and Yates, J. R. (2006) ProLuCID, a fast and sensitive tandem mass spectra-based protein identification program. *Mol. Cell. Proteomics* **5,** S174
32. Peng, J., Elias, J. E., Thoreen, C. C., Licklider, L. J., and Gygi, S. P. (2003) Evaluation of multidimensional chromatography coupled with tandem mass spectrometry (LC/LC-MS/MS) for large-scale protein analysis. The yeast proteome. *J. Proteome Res.* **2,** 43–50
33. Tabb, D. L., McDonald, W. H., and Yates, J. R., 3rd. (2002) DTASelect and Contrast. Tools for assembling and comparing protein identifications from shotgun proteomics. *J. Proteome Res.* **1,** 21–26
34. Bimboese, P., Gibson, C. J., Schmidt, S., Xiang, W., and Ehrlich, B. E. (2011) Isoform-specific regulation of the inositol 1,4,5-trisphosphate receptor by *O*-linked glycosylation. *J. Biol. Chem.* **286,** 15688–15697
35. Hoppins, S., Lackner, L., and Nunnari, J. (2007) The machines that divide and fuse mitochondria. *Annu. Rev. Biochem.* **76,** 751–780
36. Yoon, Y., Krueger, E. W., Oswald, B. J., and McNiven, M. A. (2003) The mitochondrial protein hFis1 regulates mitochondrial fission in mammalian cells through an interaction with the dynamin-like protein DLP1. *Mol. Cell. Biol.* **23,** 5409–5420
37. Hart, G. W., Slawson, C., Ramirez-Correa, G., and Lagerlof, O. (2011) Cross-talk between *O*-GlcNAcylation and phosphorylation. Roles in signaling, transcription, and chronic disease. *Annu. Rev. Biochem.* **80,** 825–858
38. Wang, Z., Gucek, M., and Hart, G. W. (2008) Cross-talk between GlcNAcylation and phosphorylation. Site-specific phosphorylation dynamics in response to globally elevated *O*-GlcNAc. *Proc. Natl. Acad. Sci. U.S.A.* **105,** 13793–13798
39. Hui, L., Hong, Y., Jingjing, Z., Yuan, H., Qi, C., and Nong, Z. (2010) HGF suppresses high glucose-mediated oxidative stress in mesangial cells by activation of PKG and inhibition of PKA. *Free Radic. Biol. Med.* **49,** 467–473
40. Singh, L. P., and Crook, E. D. (2000) Hexosamine regulation of glucose-mediated laminin synthesis in mesangial cells involves protein kinases A and C. *Am. J. Physiol. Renal Physiol.* **279,** F646–654
41. Hatakeyama, H., Kishimoto, T., Nemoto, T., Kasai, H., and Takahashi, N. (2006) Rapid glucose sensing by protein kinase A for insulin exocytosis in mouse pancreatic islets. *J. Physiol.* **570,** 271–282
42. Chang, C. R., Manlandro, C. M., Arnoult, D., Stadler, J., Posey, A. E., Hill, R. B., and Blackstone, C. (2010) A lethal *de novo* mutation in the middle domain of the dynamin-related GTPase Drp1 impairs higher order assembly and mitochondrial division. *J. Biol. Chem.* **285,** 32494–32503
43. Frank, S., Gaume, B., Bergmann-Leitner, E. S., Leitner, W. W., Robert, E. G., Catez, F., Smith, C. L., and Youle, R. J. (2001) The role of dynamin-related protein 1, a mediator of mitochondrial fission, in apoptosis. *Dev. Cell* **1,** 515–525
44. Gu, Y., Ande, S. R., and Mishra, S. (2011) Altered *O*-GlcNAc modification and phosphorylation of mitochondrial proteins in myoblast cells exposed to high glucose. *Arch. Biochem. Biophys.* **505,** 98–104
45. Buse, M. G. (2006) Hexosamines, insulin resistance, and the complications of diabetes. Current status. *Am. J. Physiol. Endocrinol. Metab.* **290,** E1-E8
46. Karunakaran, U., and Jeoung, N. H. (2010) *O*-GlcNAc Modification. Friend or Foe in Diabetic Cardiovascular Disease. *Korean Diabetes J.* **34,** 211–219
47. Tanaka, Y., Konno, N., and Kako, K. J. (1992) Mitochondrial dysfunction observed in situ in cardiomyocytes of rats in experimental diabetes. *Cardiovasc. Res.* **26,** 409–414